The structure of composite rollers with iron or nickel-iron base and hard surface layer of WC or TiC based hard alloy produced by the method of hot vacuum pressing with a liquid phase

Vladislav Kaverinskiy [a]*, Zoya Sukhenko [a]

[a] Department of Abrasion- and Corrosion-Resistant Powder Construction Materials, Frantsevich Institute for Problems of Materials Science, Krzhizhanovsky str., 3, Kiev-142 03680, Ukraine

* Corresponding author, Tel.: +38-050-212-17-24, e-mail address: insamhlaithe@gmail.com

A R T I C L E   I N F O

K E Y   W O R D S

A B S T R A C T

In this work the structure and properties of composite rollers with surface layer made of hard alloy were studied. The rollers were made by the powder metallurgy method with sintering during pressing and the presence of a certain liquid phase during sintering (semi-liquid sintering). WC-Co and TiC-Ni-Fe materials were used as hard alloys. Iron-carbon and iron-nickel materials were used as soft base. All of the composite layers were formed in one process. The structure of base materials and border layer of these composites were studied. Investigations of thermocycling sustainability of these composite samples were carried out.

1. INTRODUCTION

The working equipment of high-speed rolling mills is made of high-strength hard alloys based on tungsten carbide (with 15-25 % of WC). Idler (directive) rollers do not bear a high stress, but since they are subject to wear, at such high speeds, they are also made of hard alloy [1]. But there is an idea to only make the surface of the hard alloy, while the base is made of a softer and cheaper material [2]. This approach could both reduce the price of such rollers material and simplify their inner surface tooling for precise fit when fitting onto a shaft. Thus, we have a two-layer composite material in which one layer is made of a hard alloy and the other of an alloy based on iron or nickel. The peculiarity of this material is that it is made during one cycle by the method of powder metallurgy. Another feature of the material being studied is that it is manufactured by the method of hot vacuum pressing

with a certain amount of a liquid phase presence. This allows the material to be non-porous, and therefore having higher mechanical properties [3]. Structure peculiarities of this kind of materials seemed to be interesting to study.

The aim of this research is to investigate structure peculiarities of Fe-C and Fe-Ni middle layer and its joint zone with WC and TiC based hard alloy layer in idler rollers produced by the method of hot vacuum pressing with liquid phase and to study resistance of such material to thermal cycles with rapid cooling.

2. RESEARCH MATERIAL AND METHODOLOGY

For the product manufacture a method of hot vacuum pressing was used. This method of powder metallurgy combines pressing and sintering in a single cycle. The temperature of the process is set to make some amount of

liquid phase. Under pressure, this liquid phase comes to pores and fulfills them. But during the pressing nickel-iron alloys, no liquid phase appeared because of the short interval between liquidus and solidus and higher melting temperature. There is no liquid phase most of the pressing and sintering time. But in the end of the process the temperature and the pressure are raised.

The next materials were made:
- composite of iron-carbon alloy and hard alloy based on TiC with Ni-Fe matrix;
- composite of iron-nickel alloy and hard alloy based on TiC with Ni-Fe matrix;
- composite of iron-nickel alloy and hard alloy based on WC with Co matrix

Iron-nickel alloy consisted of 45 % of Ni and 55 % of Fe. Iron-carbon alloy has about 3 % of C. The composition of the hard alloy based on TiC with Ni-Fe matrix is 50 % of TiC, 25 % of Ni and 25 % of 25 % Fe. Hard alloy based on WC with Co matrix contains 15 % of Co and 85 % of WC.

As the raw materials, the following powders were used: carbonyl iron powder (particles size ≤ 5 μm), electrode graphite chips, carbonyl nickel powder (particles size 1 – 3 μm), cobalt powder (particles size 1 – 5 μm), WC powder (particles size ≤ 3 μm), and TiC powder (particles size ≤ 3 μm).

The powders had following chemical impurities: carbonyl iron: C – 0.014 %, Mn – 0.021 %, Si – 0.029 %, P – 0.009 %, S – 0.012 %, Cu – 0.018 %; carbonyl nickel: Fe – 0.006 %, C – 0.08 %, O – 0.07 %, S – 0.0004 %; graphite: mineral impurities (SiO_2, Al_2O_3, MgO) with their total amount not more that 1.6 %; tungsten carbide: C (graphite) – 0.04 %, O – 0.44 %, N < 0.002 %, others (Fe, Cu, Mo, Cr, Ti together) – 0.023 %; titanium carbide: C (graphite) – 0.02 %, O – 0.37 %, N < 0.002 %, others together – 0.018 %.

The graphite powder was obtained from recycled electrodes by their mechanical crushing to a rough powder (up to hundreds microns) and then it was mixed with carbonyl iron powder and the powder mixture was milled in a ball mill (МШ-100Д) with WC grinding balls (ball diameter ~12 mm) to the state with up to 40 – 50 μm. For the hard alloys, manufacture carbide powders (WC or TiC) were mixed with Co or Fe and Ni powders correspondently and the mixture was milled in the ball mill (as above). The structure of the powders after milling was hard particles (WC or TiC) with the soft component (Co or Fe/Ni) smeared on them. The ball mill has a working volume of 100 dm³. The inner surface of the mill drum is lined with carbide plates. The diameter of the inner cylindrical surface of the mill is 0.5 m. The drum of the mill rotates at a frequency of 36 rpm. A total weight of grinding balls is 300 kg. Denatured alcohol with small impurities of benzene and other hydrocarbons was used as the grinding liquid. The time of grinding process was about 24 hours for all cases. After discharging, the milled mixtures were vacuum-dried for about 6 hours. The loss of material after milling process was not more than 5 %.

The pressing and sintering process was carried out in graphite molds. To simplify the product removal and to protect of carbon diffusion, the boron nitride suspension coating of the inner mold surface was applied into the material. For the mold coating, a solution of 150 g BF-2 glue in 1 l of acetone was used in which boron nitride powder is stirred (50 g boron nitride for 0.25 l of the glue solution).

For the composite of iron-carbon alloy / hard alloy based on TiC with Ni-Fe matrix the pressing process was carried out in two main steps: producing of outer layer blank and pressing/sintering process of inner layer with the prepared outer layer blank. This is because Fe-graphite and TiC-Fe-Ni alloys need different sintering regimes. The technological scheme of the temperature and pressing force changing during the process is given as a plot in Figure 1. The temperature was measured by a tungsten-rhenium thermocouple. It should be noticed that the temperature shown is so called "technological temperature" measured with a thermocouple put in one place of the sintering/pressing facility. The real temperature inside the mold might have some variations compared with the measured values but should be close to them.

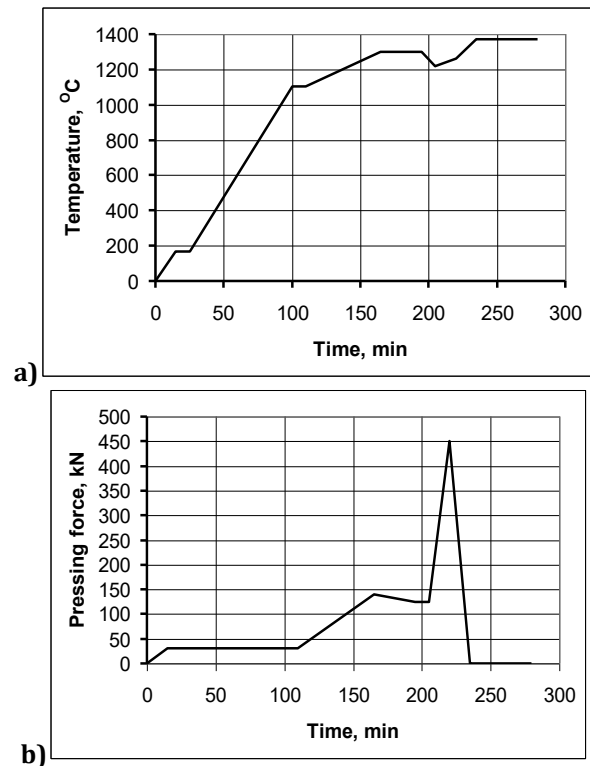The pressing chamber was evacuated.

a)

b)

Fig. 1. Technological scheme of temperature (a) and pressing force (b) changing during the outer layer blank (TiC with Ni-Fe matrix) producing process for composite of iron-carbon alloy and hard alloy based on TiC with Ni-Fe matrix

The temperature/pressing force regime of the process was specially developed to obtain some amount of liquid phase. By the moment the liquid phase is supposed to occur, the pressing force is raised to fill the porosity. Then, which is the peculiarity of the technique, the temperature is to decrease by about 80 °C and the pressing force is extremely raised which leads to a dense, non-porous material obtaining. The final stage is annealing without pressure.

The surface (especially inner) of the obtained outer layer blank, which is a TiC-based hard alloy ring, is enabled to minor machining. After that, it is set into a mold again. Also a graphite kernel coated with the boron nitride suspension is placed to the center of the mold to form the central hole. The space between the center kernel and the outer layer blank is

filled with the prepared powder mixture of iron and graphite. Between the bottom as the top puncheon and the processed material, plates of low-carbon steel are placed also coated with the boron nitride to prevent their welding to the product. These plates prevent the additional carbon diffusion to the material from graphite puncheons.

The goal was to obtain a non-porous structure of the inner layer similar to the cast-iron, but not to the iron-graphite sintered porous materials used as anti-friction. Compared with known for hard alloys semi-liquid sintering processing such technique applied to iron-graphite alloys was not obvious. Thus the four different regimes were investigated. The idea was to heat the material to the temperature close to, but below the solidus, keep in that state for some time under pressure to obtain maximum possible sealing, then to raise temperature closer to solidus and raise the pressure. The technological schemes of temperature and pressing force changing during the process of the composite roller manufacture are given as plots in Figure 2. For the temperature regimes only higher parts are given to make the most important section more readable. The pressing regime (Figure 2 – b) was the same for all of the cases.
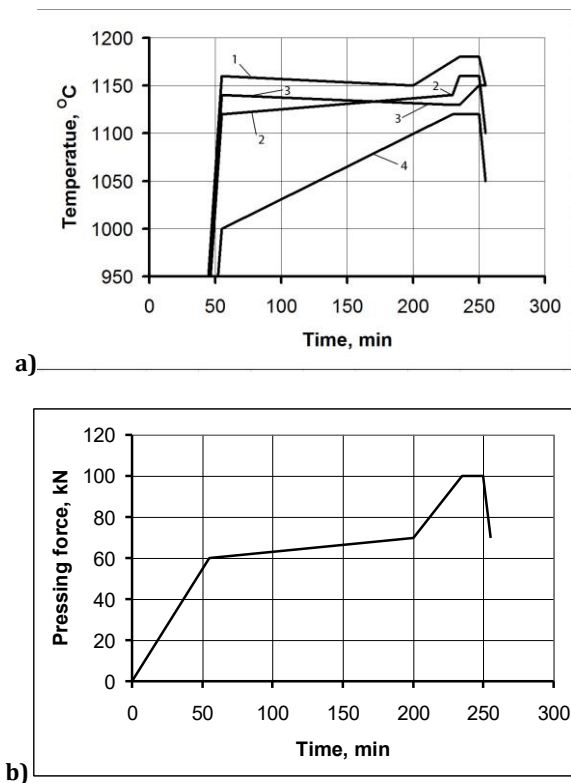

a)

b)

Fig. 2. Technological schemes of temperature (a) and pressing force (b) changing during producing process for composite of iron-carbon alloy and hard alloy based on TiC with Ni-Fe matrix (inner layer formation)

The pressing process consists of the following stages: raising of the pressing force to the working values during heating, long exposure in conditions of slow and slight increase of the pressing force (the temperature at this stage changes insignificantly and decreases or increases depending on the certain regime), comparatively short but significant increase of the pressing force as the temperature rises.

For rollers with iron-nickel alloy inner section, both layers were formed in one stage of sintering. Powder fills mold cavity in two layers. Only short pre-pressing was performed for outer layer for keeping its shape during filling the mold with powder for inner layer. The technological regime of pressing and sintering for the rollers with iron-nickel alloy inner section and hard outer layer of hard alloy based on TiC with Ni-Fe matrix was the same as shown in Figure 1 previously (as it was for alloy based on TiC with Ni-Fe matrix). For rollers with outer layer of hard alloy based on WC with Co matrix, this regime was somewhat different, as it is shown in Figure 3.
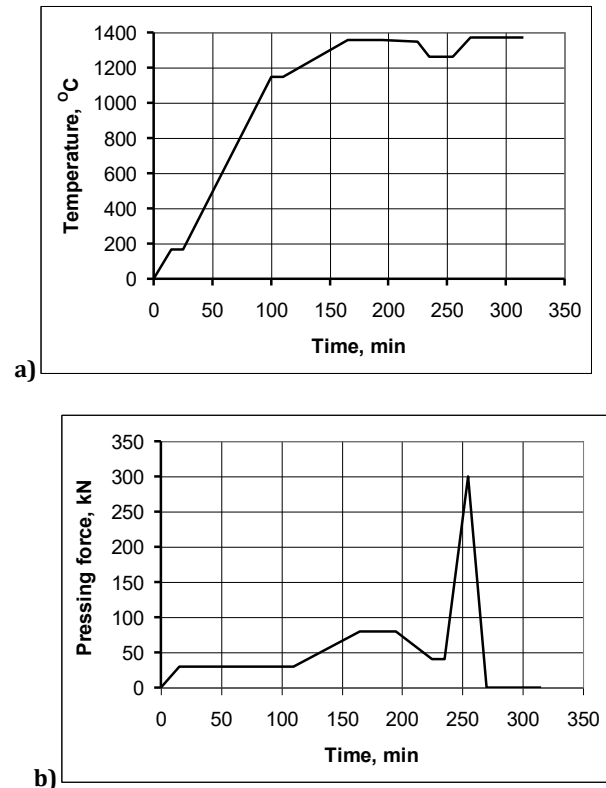

a)

b)

Fig. 3. Technological scheme of temperature (a) and pressing force (b) changing during producing process for composite of iron-nickel alloy and hard alloy based on WC with Co matrix

This technique is also aimed at some amount of liquid phase obtaining and extremely raising of pressure force to fill the porous.

Rolls with outer diameter of 80 mm and inner diameter of 25 mm were pressed and sintered for this study.

For the detection of the initial microstructure, samples of iron-nickel and iron-carbon alloys with hard alloys were subjected to metallographic analysis. For the metallographic samples etching, the following chemical agent were used:

4 % solution of HNO_3 in ethanol (for Fe-C iron-carbon alloy), 15 % water solution of $FeCl_3$ (for iron-nickel alloy), and 15 % water solution of Na_2S_2O for color etching of ferrite. Diamond pastes were used for polishing. For all samples, hardness was measured by the Rockwell method.

To estimate the stability of the compositions to thermal shock, thermal cycling tests were carried out. The samples were heated in the flame of a gas burner to a pale red glow

($\sim 500°C$) and cooled in salt water (7 – 10 % of NaCl). Heating and cooling cycles were continued until a crack appears. Micro hardness measurement was performed in the area near the crack and neat the joint zone. Metallographic analysis was used to study the structure state after thermal cycling and crack appearance.

To study the consistency of thermal expansion coefficients, dilatometric tests of the iron-nickel alloy were carried out.

3. RESEARCH RESULTS AND DISCUSSION

Primary interest was given to the structure of the components of the soft basis of compositions (iron-carbon and iron-nickel alloys). The microstructure of various samples of iron-carbon material is presented in Figure 4 and Figure 5.
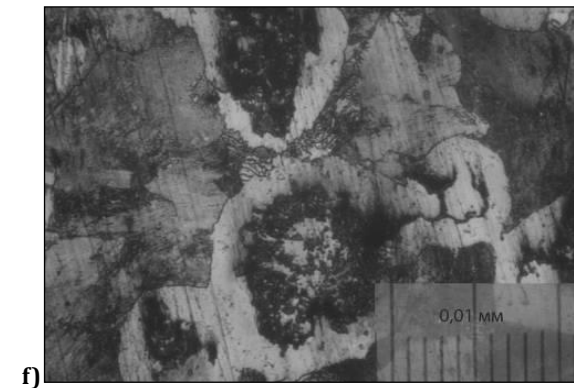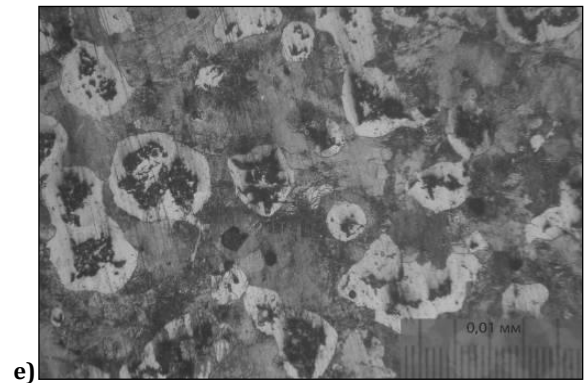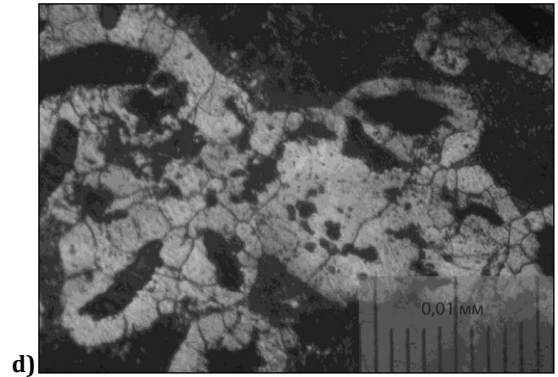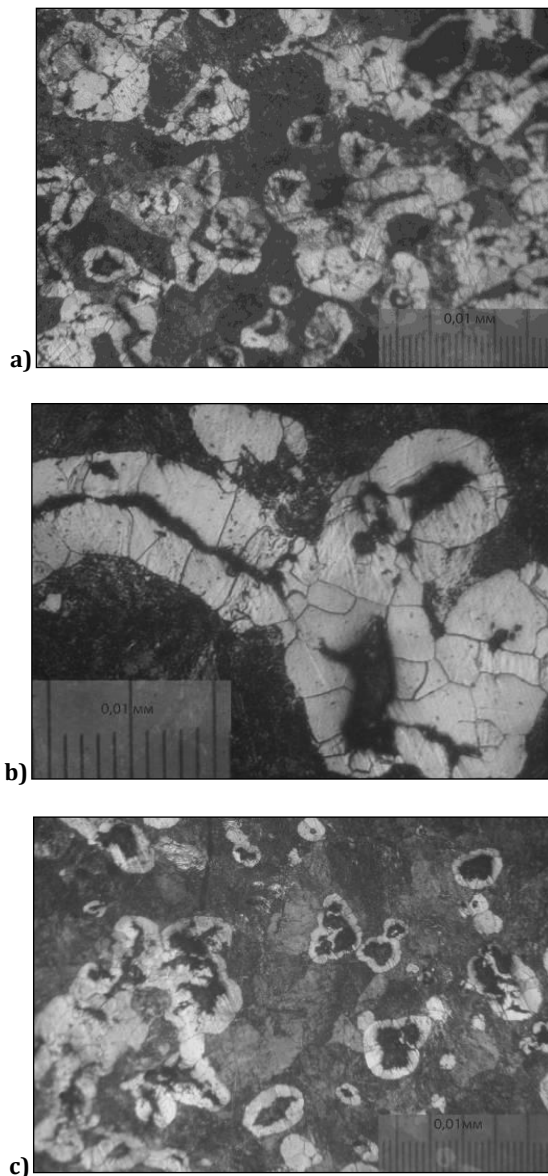

a)

b)

c)

d)

e)

f)

Fig. 4. Microstructure of non-pores iron-graphite material manufactured by regimes 1 – 3: a), c), e) magnification ×100; b), e), f) magnification ×250

Photographs of Figure 4 (a, b) – regime 1, (c, d) – regime 2, and (e, f) – regime 3 were taken from three different samples manufactured by different regimes. The structure of a sample manufactured by regime 4, which is quite different, is shown in Figure 5.

Ordinary sintered iron-graphite composites have a porous structure [4]. As can be seen from the above photographs of the microstructure, the iron-graphite material obtained by the powder metallurgy method, but with the use of vacuum pressure and sintering in the presence of a liquid phase, can have a structure similar to a ferritic-pearlitic cast iron structure. The shape of graphite in this material is somewhat specific and it depends on the sintering regime. Graphite is represented by particles close to the spherical, lamellar and elongated shape. In some cases, graphite is represented by fragmented clusters of mostly rounded shapes that are surrounded by ferrite sections. An

interesting feature is the presence of a ferrite in the central part of fragmentation graphite aggregates – they seem to be torn from the inside. Such fragmented graphite inclusions are mostly observed in the samples manufactured by regime 3. Formation of this "torn from the inside" shape can be explained as follows: initial graphite particles are spongy (porous), the liquid phase contacting with them penetrates to these micro pores, penetrating into the particle structure, the liquid phase breaks them from the inside. In conditions of higher temperatures and longer and longer exposure in them, recrystallization of graphite through the liquid phase occurs, so then they take spherical or flaky shape. Graphite inclusions of elongated shape seem to be secondarily precipitated from the liquid phase locally supersaturated with carbon (as in pig iron).
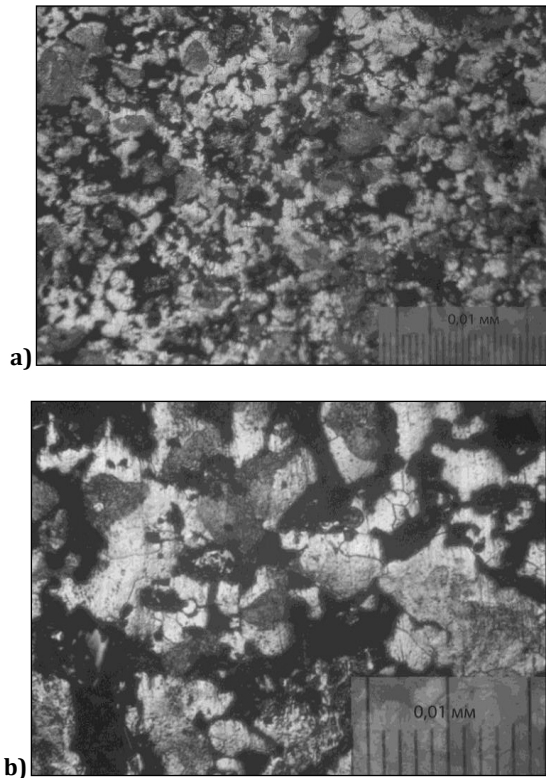

Fig. 5. Microstructure of pores iron-graphite material manufactured by regime 4: a) magnification ×100; b) magnification ×250

A comparison of the contemplative metallographic results allows us to conclude that the structure of samples obtained by regime 2 (Figure 4 – c, d) seems to be slightly better than that of regime 1 (Figure 4 – a, b). In the structure of samples obtained by regime 1 there are more elongated secondarily precipitated graphite inclusions with a quite big part of the ferrite surrounding them. The structure of the samples obtained by regime 2 is very close to the structure of nodular cast iron with pearlitic matrix. But this nodular cast iron was obtained without any Mg alloying used for this purpose in cast materials. The structure of the sample manufactured by regime 3 (further sample 3) has above described specific "torn from the inside" graphite inclusions shape and the highest part of pearlite (estimated from 10 photos from various samples). Also for some reasons, the difference in the shapes of the graphite inclusions might be additionally

associated with the shape of the particles of the initial powder. However, in bare outlines, the difference in structures of the samples 1 – 3 is not very significant, but the same could not be said on the sample 4, which typical structure is presented in Figure 5.

The characteristic feature of the structure of the sample 4 is the presence of strong porosity and low part of pearlite. This structure is somewhat close to that of porous iron-graphite antifriction alloys. Since for wear-resistant bimetallic compositions, it is optimal to obtain a non-porous material with a structure of cast iron, the structure obtained in sample 4 is not suitable for this purpose. The cause of such a structure is relatively lower sintering temperature and, because of this fact, lack of liquid phase to fulfill the pores.

For the samples, quantitative metallographic investigation also has been carried out. The average characteristics of their microstructure for the samples obtained by regimes 1 – 3 are given in Table 1.

Table 1, Average characteristics of iron-graphite material obtained by hot vacuum pressing in the presence of a liquid phase

Volume fraction of structural components %			Size of the graphite particles, µm	Average ferrite grain size, µm	Hardness, HB
Ferrite	Pearlite	Graphite			
23.5 – 34.5	37.4 – 68.6	7.9 – 13.2	6,3 – 86,4	38,6	140 – 156

Graphite particles are surrounded by ferrite sections, the average grain size of this ferrite is 38.55 µm. Porosity is completely absent. The presence of the liquid phase in the process of sintering is confirmed by the lack of porosity, the presence of ferrite around the graphite inclusions. The incontrovertible evidence of the liquid phase presence both in hard alloy and iron-carbon alloy were liquid phase leaks, which look like small metal drops emerged from the mold gaps during pressing process.

There is a statistically significant but not radical difference in the structure parameters of the samples 1 – 3. Here are the average values:
Sample 1:
– ferrite: 34.5 %
– pearlite: 52.3 %
– graphite:13.2 %
– graphite inclusions size: 33.8 µm (nodular), 86.4 µm (elongated)
Sample 2:
– ferrite – 23.9 %
– pearlite – 63.9 %
– graphite – 12.2 %
– graphite inclusions size: 32.2 µm (nodular), 62.2 µm(elongated)
Sample 3:
– ferrite – 23.5 %
– pearlite – 68.6 %
– graphite – 7.9 %
– graphite inclusions size ("shards"): 6.3 – 17.7 µm
– graphite agglomerates diameter: 67 µm
The structural characteristics of sample 4 are as follows:

– ferrite – 24.6 %
– pearlite – 37.4 %
– graphite + pores – 38 %
– pores size – 35.2 µm %

So we can see that the sample 3 has the biggest part of pearlite and the sample 1 has the lowest, but the sample 1 is the most ferritical. Sample 1 has more elongated graphite inclusions, but the average diameters of nodular ones are almost same. The size of "sharded" graphite inclusions in sample 3 is several times smaller than the diameter of the inclusions in other samples, but the graphite agglomerates diameter is two odd times bigger than nodular inclusions of others samples.

Also the samples hardness was measured. The range of its average values is given in Table 1. Also there was some difference between the samples. Its values are following:

Sample 1: 140±3.6 HB
Sample 2: 153±8.0 HB
Sample 3: 156±4.7 HB
Sample 4: 146±4.5 HB

The highest hardness is observed in sample 3, which is owing to the highest pearlite content. Its value is close to that of sample 2, but the hardness of sample 3 has less value scatter. Such factors as higher part of ferrite in sample 1 and porous of sample 4 make their hardness significantly lower.

Thus, the regimes 2 and 3 described above seem to be more optimal that 1 and surely 4. The samples obtained by regime 4 have high level of porous, which is unacceptable according to the objective. Samples 2 and 3 are more pearlitic, harder and have less ductile shaped graphite inclusions than sample 1. Hence they may have higher wear resistance, which is crucial for these products. It would be too arrogant to say that regime 2 or 3 is better. These samples properties are quite close, but there is a rather significant difference in their structure. The more nodular shape of graphite inclusions in sample 2 may provide greater strength and impact strength, as in nodular iron, but the flaked shape of inclusions in sample 3 could provide better vibration damping, as in ductile (malleable) iron. Assuming the fact that these regimes are close enough, an averaged sintering regime between them could be provided. The scheme of such a regime (temperature changing per time) is shown in Figure 6.
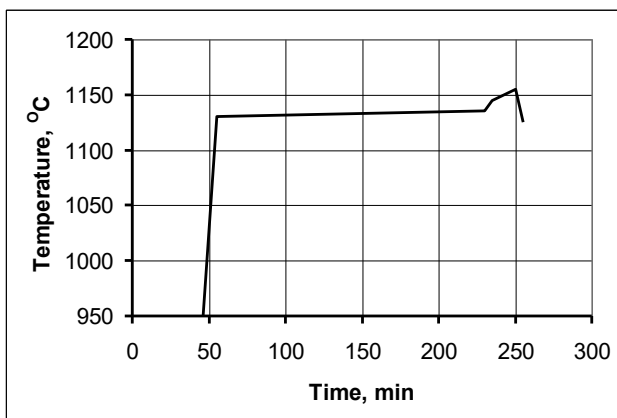

Fig. 6. A proposed technological scheme of temperature changing during producing process of iron-carbon alloy for composite with hard alloy (inner layer formation)

The hardness of the iron-nickel alloy obtained by the method of hot vacuum pressing was 360 – 370 HB. Microstructures of iron-nickel alloy are shown in Figure 7.

It should be noted that in all volume of iron-nickel alloy there are areas of both individual carbide inclusions and their conglomerates (Figure 7a). The measurement of the microhardness of such conglomerates has shown that it coincides with the hardness of a hard alloy. The presence of these structural components is related to the input of tungsten carbide powder into the initial charge to increase the alloy's hardness.
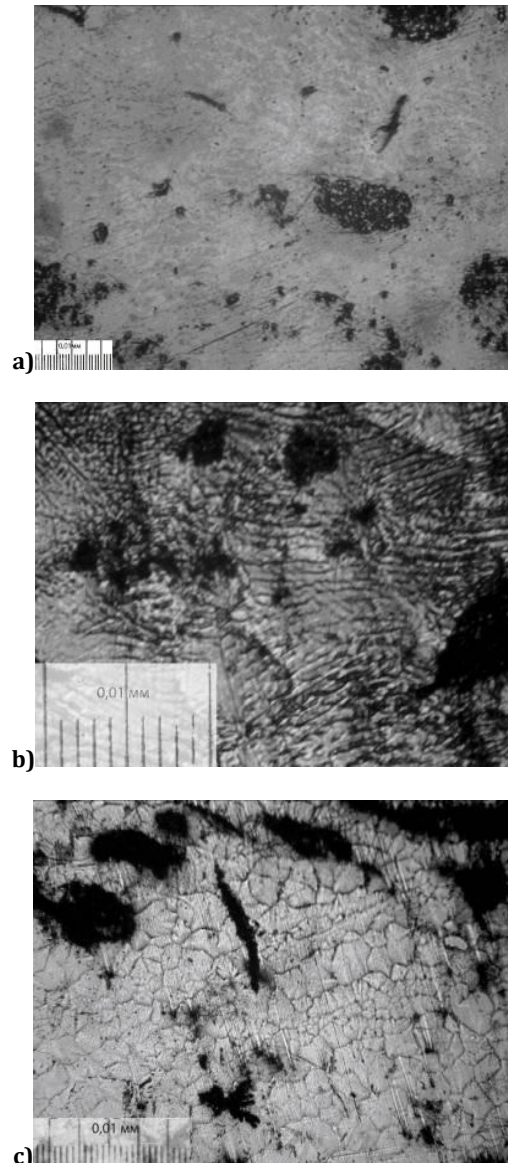

a)

b)

c)

Fig. 7. Microstructure of iron-nickel alloy obtained by the method of hot vacuum pressing: a) not etched sample, magnification ×50; b) etching in a solution of bleach, magnification ×250; c) etching in a solution of bleach, magnification ×100

Figure 7 (b) shows the microstructure of iron-nickel alloy, found by etching in a solution of chlorine iron. As can be seen from Figure 7 (b), in some parts of the iron-nickel alloy, layered structures are observed, structurally similar to eutectic or eutectoid. In the joint zone and in some separate

sections in the depth of the alloy (Figure 7c) layered structures are not detected. Perhaps the presence of such structures is associated with the implementation in the process of production of iron-nickel alloy eutectoid transformation in it [5].

The measurement of micro hardness showed that the micro hardness of zones having a layered structure is 595 ± 30 N/mm², the sections which an even-axial structure have hardness 517 ± 59 N/mm². The comparison of averages with known variances showed that the difference in the mean can be considered as significant with a reliability of 95%. Thus the layered structures have slightly higher hardness.

Hard alloy layer of the composite had an ordinary structure. We will not focus on it.

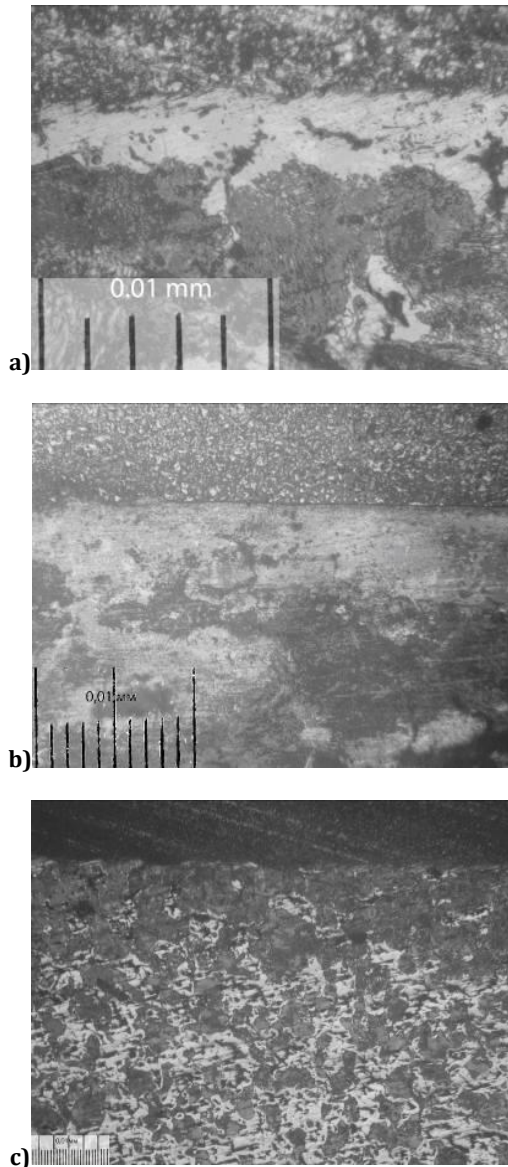Figure 8 shows the microstructure of the joint "iron-graphite material/hard alloy".

a)

b)

c)

Fig. 8. Microstructure of the joint zone of the "iron-graphite material / hard alloy" sample: a) chemical etching in a 4% solution HNO₃, magnification ×500; b) etching in a 15% solution of sodium thiosulfate, magnification ×200; c) etching in a 4% solution HNO₃, magnification ×50
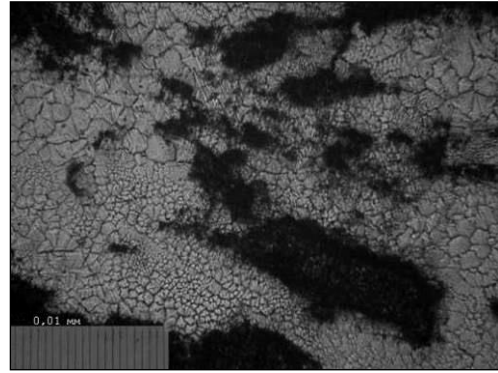

Fig. 9. Microstructure of the transition zone of the sample of the composition "iron-nickel alloy (45% Ni) / hard alloy based on titanium carbide" (magnification ×100)

The study of the transition zone in the composition of "iron-graphite material / hard alloy" showed that the iron-graphite alloy in it has a structure of gray iron with a fairly high content of pearlite and relatively low content of graphite. Sometimes it is possible to note the blurriness of the border, which indicates the presence of diffusion. In the place of the breakthrough, hammered by the impact of the hammer ($\sim$ 400g), there is no cracking at the material junction. On the whole number of microphotographs of the transition zone, a band of light phase along the interface with a width of 17.2 ± 5 μm is observed.

A research was conducted to detect the phase nature of the aforementioned light strip along the materials interface. Since we were dealing with an iron-carbon alloy, this band could theoretically be represented by ferrite, cementite or austenite. In order to establish, what it really is, the measurement of micro hardness and characteristic etching in 15% solution of sodium thiosulfate was carried out, which paints ferrite [6].

Studies of micro hardness showed that the micro hardness of the light strip along the interface is 1815.4 ± 34 N/mm². At the same time, the hardness of the ferrite in the material's depth was 1096 ± 27 N/mm², the perlite's hardness was 1835 ± 91 N/mm². Thus, we can draw the conclusion that the lighter phase along the boundary is not a cementite, while its hardness far exceeds the hardness of the ferrite in the depth of the material. Etching in a 15% solution of sodium thiosulfate stained this band, thereby showing that it is ferrite (Figure 8b). High hardness of this ferrite in the transition zone is obviously due to a strong slander due to the difference in the coefficients of thermal expansion of materials and the doping of this ferrite due to diffusion in the transition zone. The reason for the appearance of ferrite along the material boundary may be diffusion of carbon from iron into the hard alloy layer. Studying of the sample in small magnification, however, showed that the number of pearlite gradually decreases with the distance from the transition zone (Figure 8c).

Study of the microstructure of the joint zone in the specimens of the "iron-nickel alloy (45% Ni) / hard alloy based on titanium carbide" composition showed that, as it can be seen from Figure 9, grains of iron-nickel alloy are significantly finer near the interface border.

Possible reasons for grains grinding in the transition zone could be the effects associated with slander as a result of the alternating stress. In order to find out the reasons for

grinding grain in the transition zone, a sample consisting of iron-nickel alloy and hard alloy based on titanium carbide was subjected to recrystallization annealing at 600°C for two hours. Figure 10 shows a photograph of the joint zone of the sample after annealing.

Fig. 10. Microstructure of the transition zone of the sample of the composition "iron-nickel alloy (45% Ni) / hard alloy based on titanium carbide" after annealing at 600 ° C for two hours (magnification ×100)

Figures 9 and 10 show that recrystallization annealing led to the disappearing of small grains near the joint and the consolidation of the structure near the interface. Thus, before annealing the average conditional grain size at a distance of 0.2 mm from the interface was 11±4 μm, after annealing it was 45±12 μm . The grain size in the main material in the initial state was 46±16 μm. It follows that the grinding of the structure clearly associated with slander near the interface.

After and before annealing the micro hardness was measured of the material near the joint layer. The distance where micro hardness has been measured was not greater than 0.3 – 0.45 mm from the interface line. The measurement showed that the micro hardness of the iron-nickel alloy in this zone was 616 ± 29.8 N/mm^2; at the same time, the microhardness in the bulk of the iron-nickel alloy was 559±15.1 N / mm^2. Thus, the iron-nickel alloy in that area has a high hardness, which may be due to diffusion processes that took place during pressing and sintering of the sample and stress hardening. It was found that the values of micro hardness increase coming closer to the interface. On the distance closer than 0.05 mm the hardness can be more than 700 N/mm^2. However, on the distance of 0.20 mm its values become similar to those in the depth of the material. After the above mentioned annealing at 600°C the average micro hardness of this zone become 588±29 N / mm^2, which is less than in was before the annealing and is closer to the average micro hardness of the rest volume of the material.

Presumably, recrystallization annealing at 600°C will increase the plasticity and impact strength of the material of the transition zone in such compositions. That might increase the resistance of these compositions to thermal shock and reduce the probability of their destruction when cooling.

To estimate the stability of the composition "iron-graphite material / hard alloy" to thermal shock, thermal cycling tests were carried out. The samples were heated in the flame of a gas burner to a pale red glow (400 – 500°C) and cooled in salt water (7 – 10 % of NaCl). Salt water cools significantly faster, so the test conditions become more extreme [7]. The test for thermocycling did not lead to the destruction of the samples at the macro level. Twenty cycles were completed. In the study of the microstructure of the joint and the materials adjacent to it, after the first ten cycles, the formation of the micro cracks at the junction was noted (Figure 11a), as well as the formation of strings of graphite particles and, possibly, micro cracks in the fibrous region of iron-graphite material (Figure 11b). After twenty cycles on the iron-graphite material, cracks become visible to the naked eye. The study of the microstructure showed that cracks apparently were formed on the base of graphite chains.

Thermocycling experiment was also made with "TiC based hard alloy / Ni-Fe alloy" and "WC based hard alloy / Ni-Fe alloy" compositions. The regime of thermocycling was the same as for "iron-graphite material / hard alloy".

Thermocycling of samples showed that the compositions of iron-nickel alloy with hard alloys based on WC with cobalt matrix and one based on TiC with iron-nickel bonds have a different type of destruction. So on samples consisting of iron-nickel alloy and hard alloy with TiC after six cooling cycles there was a noticeable crack. The crack passed along the iron-nickel alloy in parallel to the interface section at the distance of 0.3-0.45 mm (Figure 12a).
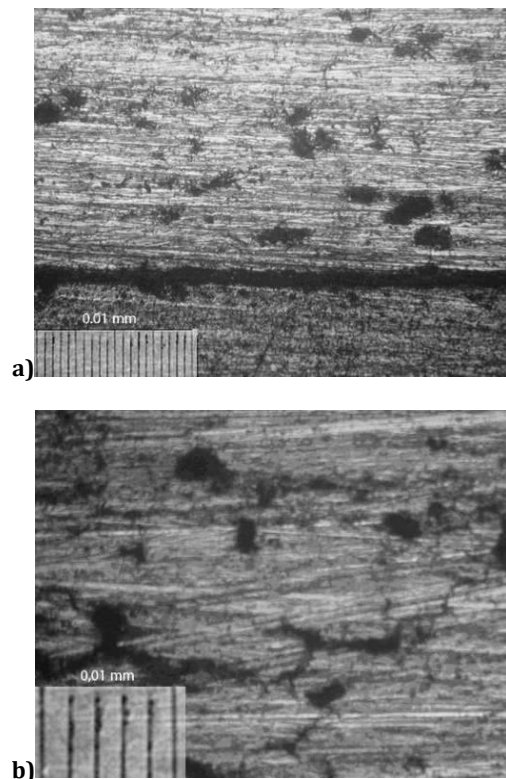

a)

b)

Fig. 11. Microstructure of the specimen of the composition "iron-graphite material / hard alloy" after 10 cycles: a) transition zone (magnification ×100); b) micro cracks (magnification ×400)

Samples consisting of iron-nickel alloy and hard alloy based on WC proved to be much more resistant to thermocycling because signs of destruction in them appeared only after the seventeenth cooling cycle. In this case, the crack went through a hard alloy perpendicular to the interface. It should also be noted that the study of the crack under a microscope showed that the peak of the crack in the junction area has a T-shaped form (Figure 12b).

The difference in the nature of fracture and resistance to thermocycling is owing to different viscosity of these hard alloys. So it can be noted that the coefficient of thermal expansion of the alloy based on WC is more consistent with the coefficient of thermal expansion of iron-nickel alloy with 45% nickel.

Dynamometric tests of iron-nickel alloy showed that at a temperature of about 400°C, a sharp change in the coefficient of linear thermal expansion was observed. This shows the plot in Figure 13.
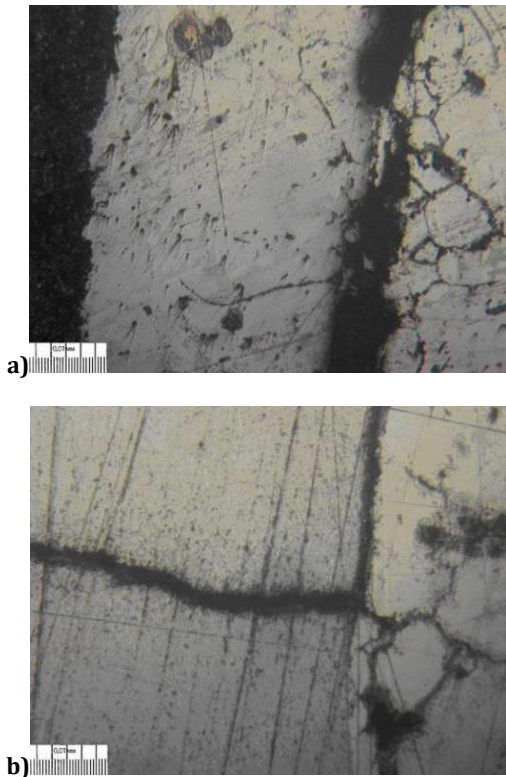

Fig. 12. View of destruction of the sample after heat cycles (magnification ×50): a) TiC based hard alloy/Ni-Fe alloy; b) WC based hard alloy/Ni-Fe alloy
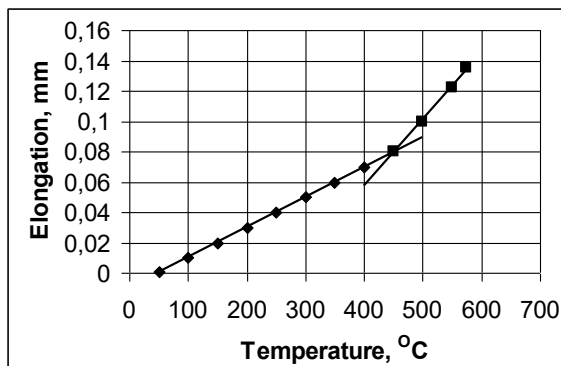

Fig. 13. Extension of the Fe-Ni alloy sample from the temperature

The value of the coefficient of linear thermal expansion in the range of temperatures 50 – 400°C is $6.829 \cdot 10^{-6}$ K^{-1}, and in the temperature range 450 – 580°C it is $14.56 \cdot 10^{-6}$ K^{-1}. The change in the coefficient of linear thermal expansion is linked with magnetic transformation that occurs in the alloy. In addition, according to some data at close temperature in the iron-nickel system eutectoid transformation is possible [5]. Observed layered structures might be signs of the second option possibility.

4. CONCLUSIONS

Samples of composite rolls were made, the outer layer of which is made of a hard alloy, and the inner (main) of a soft, less brittle and cheaper material. A notable feature of the materials of the rollers is that it is manufactured by the method of powder metallurgy by the method of vacuum hot pressing. Such material can be non-porous. As a soft base iron-carbon or iron-nickel alloys were used.

The structural features of such composite materials have been studied. It is shown that when vacuum hot pressing is performed in the presence of a liquid phase, the structure of the iron-graphite material is non-porous and resembles a cast iron structure on a pearlite basis. At the material interface, a thin layer of ferrite is observed, the hardness of which is much higher than that of ferrite in the depth of the material. The iron-nickel alloy contains both equiaxed grains and layered structures, the hardness of which is higher. The grain structure near the interface is finer. This feature is eliminated by annealing at 600°C for 2 hours.

Four different sintering regimes were investigated for the composition iron-graphite alloy / hard alloy based on TiC with Fe-graphite matrix. The desired non-porous iron-like structure was obtained through the regimes 1, 2, and 3. Among them regimes 2 and 3 give more suitable material characteristics. Basing on them an averaged sintering regime was provided, which plot is given in Figure 6. It consists of heating from initial temperature to 1130-1135°C during 55 minutes keeping this temperature for 175 minutes, then gradually raising the temperature up to 1155°C which should take a period of about 20 minutes, then going to the cooling stage without pressing. The scheme of pressing force changing during this sintering/pressing process is shown in Figure 2.

It was found that in conditions of liquid phase hot pressing/sintering of iron-graphite material, there could appear a specific graphite inclusion shape non-distinctive for cast irons. That shape is "like torn from the inside" graphite smithereens aggregates in a sphere of ferrite (see Figure 4 – e, f). Such graphite morphology could be explained by tearing of an initial spongy graphite particle when in contact with liquid iron phase. And to the end of the process it was neither solute nor recrystallized.

The stability of the developed composites for thermal cycles with sharp cooling (in salt water) was investigated. It is shown that the composite of an iron-carbon alloy and a solid TiC-based alloy with a matrix of Fe and Ni is sufficiently stable to thermocycling. For a soft base of Ni and Fe, a composite with a WC-based hard alloy is more resistant to thermal cycling than TiC-based alloy with a matrix of Fe and Ni.

Since one of the purposes was to determinate which of the studied composition is more stable to a thermal shock and thermal cycles, it could be concluded that for rollers with TiC hard alloy with Fe-Ni matrix outer layer the iron-carbon material may be a better option for inner (main) layer because according to the study, it withstands up to twenty thermal cycles before visible crack appears but the composite

with the same material of outer layer and inner one of the Fe-Ni alloy could overcome only six thermal cycles in the same conditions. However, for rollers with outer layer of WC hard alloy with Co matrix, this Fe-Ni alloy may be quite suitable material for inner layer, since it withstands seventeen thermal cycles, which is no less than the Fe-graphite alloy with the TiC hard alloy.

Because TiC based hard alloys with Fe-Ni matrix are really cheaper than expensive ones based on WC with cobalt matrix, the obtained result that the iron-graphite alloy (which is also cheaper than iron-nickel alloy) can fit the TiC-based alloy even better than Fe-Ni alloy fit WC hard alloys, seems to be also practically and economically perspective.

According to dilatometric study, the composite rollers with Fe-Ni inner layer should not be used in conditions in which their heating is greater than 400 – 450°C because of notable change in thermal expansion coefficient. While manufacturing, the cooling rate higher and close to this temperature should be slowed down, also an annealing at ~ 600°C seems to be beneficial for it reduces mechanical stress near the joint interface and removes those odd layered harder structures in the depth of material.

REFERENCES

[1] **Deshpande M.V., Saxena J.P., Kumar P., Basu S., Sebardt W.,** Development of guide roller material for steel wire-rod mill, International journal of refractory metals and hard materials, 15 (1997), 151-155.

[2] **Cassard J. J., Cassard, J., Lachenal, G., Romagnolo,** Composite guide roller for a rolling mill [Electronic resource], (1977), Resource access mode: https://patentimages.storage.googleapis.com/cd/72/b4/92b396e130b0be/US4056873.pdf

[3] **Zhigang Z. F., Oladapo O. E.,** Liquid phase sintering of functionally graded WC–Co composites, Scripta Materialia, 52 (2005), 785 – 791.

[4] **Bulanov V. Ya., Kozhevnikov V. I., Pluzhnikov V. A.,** Structure and properties of iron-graphite materials alloyed with nickel and phosphorus, Soviet Powder Metallurgy and Metal Ceramics, 6 (1967), 208 – 210.

[5] **Lyakishev N.P.** Diagrams of the state of double metal systems: Handbook. Vol. 2., Mechanical engineering, Moscow (1996). (in Russian)

[6] **Van Der Voort G. F.** *Metallography principles and practice*, ASM International, New York (1999).

[7] **Novikov I.I.** Theory of heat treatment of metals, Metallurgy, Moscow 1986. (in Russian)